ON GRANT NAG 5 1890

To: NASA Scientific and Technical
      Information Facility,
      Accession Dept.
      800 Elkridge Landing Road,
      Linthicum Heights, MD 21090

February, 8 1993

G R A N T

IN-33-CU

145-585

P-11

From: Dr. Marina Turchinskaya
       1131 University Blvd. W,
       Apt. 1912
       Silver Spring, MD 20902

FINAL REPORT

Studying the Kinetics of Magnetization in High Tc Superconductors

We report the first microscopic maps of magnetic induction in $YBa_2Cu_3O_{7-x}$ crystals which directly show the dependence of flux flow on twin density and polytwin block and twin boundary orientation. These maps were obtained by means of a recently-improved magneto-optical imaging technique. Pinning was lowest in untwinned regions and increased with increasing twin density. Anisotropy in twin boundary pinning, defined as the ratio of the magnetic induction gradient across twin boundaries to that along twin boundaries, was 10 at 17 K; this ratio increased with increasing temperature. In polycrystals, twin boundaries also had a strongly anisotropic effect on flux flow into a grain from a grain boundary.

The effect of twin structure on the superconducting properties of the high-temperature superconductor $YBa_2Cu_3O_{7-x}$ (YBCO) has been the subject of intensive study. The interaction between flux vortices and plane-parallel, {110}-type twin boundaries (TBs) determines the pinning strength of TBs which, in turn, may affect flux flow dynamics. Prior experimental investigations probing the effect of TBs on flux pinning by macroscopic measurements have yielded contradictory results. Magnetization measurements[1-3] on YBCO single crystals in the twinned and detwinned states demonstrated that TBs provide substantial pinning at certain temperatures and applied magnetic fields (H_a). However, in other studies, twin density was found to have little or no effect on pinning in single crystals[4] or thin films.[5] Results of investigations wherein the direction of vortex motion and the orientation of vortices (aligned along H_a) relative to TBs and the crystallographic axes were well-established also appear to be inconsistent. It was first reported that, for temperatures below[6] 70 K or[7] 85 K, flux penetration was easier (i.e., pinning was lower) when vortices moved along the direction of TBs ($H_a \parallel c \parallel TB$) than when they crossed TBs; a subsequent study supported the opposite conclusion.[8] Measurements of magnetic torque[9] at 76 K and resistivity near the superconducting transition temperature[10] demonstrated that pinning was highest for $H_a \parallel TB \perp c$, although it appeared that vortices crossed TBs in one study[9] and moved along TBs in the other study.[10] The apparent contradictions in these results are due, at least in part, to the ambiguities inherent in correlating macroscopic measurements of average properties of a specimen with a microscopic twin structure.

Techniques which provide microscopic maps of flux distribution are clearly preferable to macroscopic measurement methods for correlating flux flow to twin structure and quantifying flux pinning by TBs. Maps generated by a Bitter pattern decoration technique[11-13] showed that trapped vortices were aligned in the direction of TBs in low fields (2 mTesla) applied parallel to the c-axis at 4.2 K. However, the static limitations of this technique make the study of flux motion very tedious. Real-time, dynamic flux mapping of YBCO samples has been achieved by magneto-optical imaging techniques.[14-20] Recently,

Duran et al.[19] utilized one such technique to demonstrate that TBs act as channels for flux flow and that flux flow across TBs was more difficult than along TBs.

In this Letter, we report the first microscopic maps of magnetic induction in YBCO single crystals and polycrystals which show a direct correlation of flux penetration with both twin density and structure. These maps were generated by means of a recently-improved magneto-optical imaging technique[20] described below. We found that pinning was lowest in twin-free regions and increased with increasing twin density. In a twinned region, flux penetrated preferentially along the direction of TBs. Pinning by TBs was found to be highly anisotropic: the magnetic induction gradient across TBs was ten times the gradient along TBs at 17 K. This anisotropy in pinning increased with increasing temperature. Furthermore, the depth of flux penetration into a grain of a polycrystal was greatest when TBs were normal to the {001} tilt grain boundary and decreased with increasing deviation of TBs from the normal.

The YBCO crystals were grown from Y-Ba-Cu-O melts in gold crucibles following a technique described elsewhere.[21] The crystals were subsequently annealed in flowing oxygen gas at 420°C for 110 h to obtain superconducting onset temperatures of 92 K. Crystals prepared by the present method typically contain ~ 1 mole% gold[21] occupying only the Cu(I) sites.[22] Twin structures were readily imaged in a polarized light optical microscope. Flux distribution measurements on three samples are reported in this Letter. Specimen 1 was a single crystal having a "puzzle-domain"[23] twin structure composed of finely-spaced twins configured into irregularly-shaped blocks. Each block, referred to here as a polytwin block, contained TBs of one of the two possible {110} variants. Specimen 2 was a polycrystal composed of crystals with nearly common c-axes, with {001} tilt grain boundaries between the crystals.[24] This sample was mounted and polished to obtain a flat surface perpendicular to the common c-axis. Specimen 3 was a single crystal having regions of varying twin density.

Flux distribution maps were generated by means of a magneto-optical imaging technique described in detail elsewhere.[15,20] Briefly, the measurement system consisted of a miniature liquid helium cryostat

mounted on the stage of a polarizing light optical microscope. The YBCO crystal was set on the cold finger of the cryostat. A Bi-doped yttrium-iron-garnet thin film[25] on a transparent substrate was placed on top of the crystal such that the film and a {001} facet of the crystal were in contact. After cooling the crystal in zero magnetic field, a constant external field in the range of 0 to ± 65 mTesla was applied parallel to the c-axis via an electromagnet. Above a field value that depended on temperature, flux penetrated the crystal. The magnetic field within and surrounding the superconductor induced a magnetic polarization in the garnet indicator film. This polarization led to a rotation of incident polarized light through the Faraday effect, producing an intensity map when the light reflected from the crystal/film interface was passed through crossed polarizers. This magneto-optical map or image was viewed by means of a video system attached to the microscope, permitting direct, real-time observation and recording of flux flow dynamics. Intensity was correlated to magnetic induction by in-situ calibration of the indicator film in various applied fields and at different temperatures. The images were then processed in an image analysis system to generate contour maps of magnetic induction as well as induction profiles along selected lines.

Magneto-optical images of specimen 1 at several applied fields at 35 K and the twin structure of this single crystal are shown in Fig. 1. At very low applied fields, flux did not enter the crystal due to screening effects. As H_a was increased, flux penetrated initially along the direction of TBs[26] (Fig. 1b) as indicated by the yellow "fingers" signifying flux extending into the crystal from its edges. A further increase in H_a (Fig. 1c) resulted in more flux penetration, primarily from the edges of the crystal along the direction of TBs. There was significant resistance to flux motion across TBs into an adjacent polytwin block (Figs. 1c,d). When the front of flux motion reached a polytwin block boundary which was not perpendicular to the front, it turned 90° and flux proceeded to flow along the direction of the TBs in the second polytwin block (Fig. 1c, e.g., single arrows). In cases where the polytwin block boundary was nearly perpendicular to the front (i.e., the boundary was coincident with TBs), flux flow was stopped or

greatly impeded (Fig. 1c, e.g., double arrows). Rectangularly-shaped regions where there was no easy path of entry showed remarkably little flux penetration (dark areas, Fig. 1d). The same trends in flux flow were observed in other crystals for temperatures in the range of 6 to 65 K.

A contour map of magnetic induction generated from the image in Fig. 1d is shown in Fig. 1e. The slope of the induction surface along any finite segment is the induction gradient, dB/dx, which is directly related to the resistance to flux flow or the pinning force, P. Anisotropy in TB pinning, defined as the ratio of the induction gradient across TBs (segment BC, Fig. 1e) to that along TBs (segment AB, Fig. 1e) is expressed as $P_\perp/P_\parallel$. This ratio was approximately 10 at 17 K and 65 mTesla, 20 at 25 K and 32 mTesla, and 30 at 35 K and 19 mTesla. (The applied field at each temperature was chosen so that flux penetrated along the entire line AC.) Although the gradients dB/dx both along and across TBs decreased with increasing temperature, the anisotropy in pinning, $P_\perp/P_\parallel$, increased with increasing temperature. This temperature dependence of $P_\perp/P_\parallel$ suggests that the ratio of the TB pinning forces to the sum of the other pinning forces in a YBCO crystal increases with increasing temperature.

An effect of TB orientation on flux pinning was also observed in a polycrystal (specimen 2). Flux penetrated initially along grain boundaries and subsequently spread into the two contiguous grains. The depth of flux penetration into a grain was greatest when TBs were normal to the grain boundary. As the deviation of TBs from the grain boundary normal increased, the flux penetration depth decreased, indicating increased resistance to flux flow.

Magnetic induction profiles were measured in specimen 3 (single crystal, Fig. 2a) to determine the effect of twin density on flux flow. Profiles for H_a = 14 mTesla at 53 K were measured along direction 1 in an untwinned region (Fig. 2b), direction 2 in a lightly twinned region (Fig. 2c) and direction 3 in a heavily twinned region (Fig. 2d). Both twinned regions had TBs of only one orientation. Induction gradients, dB/dx, measured from the linear sections of the profiles in Figs. 2b-d were 0.4, 0.9, and 1.3 Tesla/cm along directions 1, 2 and 3 respectively. Critical current densities, J_c, were estimated from the

induction gradients by means of a relation given by Polyanskii et al.;[27] J_c values of 0.3 x 10^4, 0.7 x 10^4, and 1.0 x 10^4 A/cm^2 were obtained for the directions 1, 2 and 3 respectively.[28] Thus pinning was lowest in the untwinned region and increased with increasing twin density. Magnetization measurements have shown that the lower critical field H_{c1} was less for a crystal in the untwinned state than in the twinned state,[7] supporting our observation that flux penetration was more difficult when TBs were present. In contrast, Duran and co-workers[19] found that flux flowed five times faster along a TB than in the surrounding untwinned material; they proposed that their results may be due to residual strains or other defects at the TB that could promote easier flux penetration. Such strains or defects could be introduced during the quenching step in their crystal growth process;[29] crystals used in the present study were cooled slowly.

Our magneto-optical images clearly show that twin structure in YBCO results in inhomogeneous flux penetration for low applied fields (up to 65 mTesla) at temperatures in the range of 6 to 65 K. Twin density, the size and number of polytwin blocks, and the orientation of the polytwin block boundaries with respect to TBs were all found to have a significant effect on flux flow. Pinning by polytwin blocks was strongly anisotropic; the anisotropy, expressed by the ratio $P_\perp/P_\parallel$, increased with increasing temperature. This temperature dependence of the anisotropy suggests that pinning by TBs becomes more important relative to other pinning sources as temperature increases. Thus, it may be possible to increase pinning and J_c in YBCO at higher temperatures by controlling the twin microstructure.

References

1. U. Welp et al., Appl. Phys. Lett. **57**, 84 (1990).

2. L. J. Swartzendruber, D. L. Kaiser, F. W. Gayle, L. H. Bennett, and A. Roytburd, Appl. Phys. Lett. **58**, 1566 (1991).

3. D. L. Kaiser, F. W. Gayle, L. J. Swartzendruber, L. H. Bennett, and R. D. McMichael, J. Appl. Phys. **70**, 5739 (1991).

4. T. R. Dinger et al., in High Temperature Superconducting Compounds: Processing and Related Properties, edited by S. F. Whang and A. Das Gupta (The Metallurgical Society, Warrendale, PA, 1989), p. 23.

5. B. M. Lairson, S. K. Streiffer, and J. C. Bravman, Phys. Rev. B **42**, 10067 (1990).

6. L. J. Swartzendruber, A. Roitburd, D. L. Kaiser, F. W. Gayle, and L. H. Bennett, Phys. Rev. Lett. **64**, 483 (1990); A. Roitburd, L. J. Swartzendruber, D. L. Kaiser, F. W. Gayle, and L. H. Bennett, Phys. Rev. Lett. **64**, 2962 (1990).

7. A. Umezawa et al., Phys. Rev. B **42**, 8744 (1990).

8. J. Z. Liu, Y. X. Jia, R. N. Shelton, and M. J. Fluss, Phys. Rev. Lett. **66**, 1354 (1991).

9. E. M. Gyorgy et al., Appl. Phys. Lett. **56**, 2465 (1990).

10. W. K. Kwok et al., Phys. Rev. Lett. **64**, 966 (1990).

11. L. Ya. Vinnikov et al., JETP Lett. **47**, 131 (1988); Solid State Commun. **67**, 421 (1988).

12. G. J. Dolan et al., Phys. Rev. Lett. **62**, 827 (1989).

13. I. V. Grigorieva, L. A. Gurevich, and L. Ya. Vinnikov, Physica C **195**, 327 (1992).

14. N. Moser et al., Physica C **159**, 117 (1989).

15. M. V. Indenbom et al., Physica C **166**, 486 (1990).

16. A. Forkl, T. Dragon, and H. Kronmuller, J. Appl. Phys. **67**, 3047 (1990).

17. E. Batalla, E. G. Zwartz, R. Goudreault, and L. S. Wright, Rev. Sci. Instrum. **61**, 2194 (1990).

18. S. Gotoh and N. Koshizuka, Physica C **176**, 300 (1991).

19. C. A. Duran et al., Nature **357**, 474 (1992).

20. L. A. Dorosinskii et al., Physica C **203**, 149 (1992).

21. D. L. Kaiser, F. Holtzberg, M. F. Chisholm, and T. K. Worthington, J. Cryst. Growth **85**, 593 (1987).

22. W. Wong-Ng et al., Phys. Rev. B **41**, 4220 (1990).

23. H. Schmid et al., Z. Phys. B - Condensed Matter **72**, 305 (1988).

24. F. W. Gayle and D. L. Kaiser, J. Mater. Res. **6**, 908 (1991).

25. This novel magneto-optical indicator film[20] has in-plane magnetic anisotropy which gives higher spatial resolution (2-4 μm) and higher magnetic field saturation values than those attainable in films with normal magnetic anisotropy which are commonly used in magneto-optical measurement systems.[15,18,19] In addition, the in-plane film yields dual color maps wherein color indicates field direction and intensity is directly related to magnetic field strength.

26. Significant flux creep over a period of seconds was observed for H_a > 14 mTesla at 35 K and for lower applied fields at higher temperatures. The flux distributions shown in Figs. 1 and 2 were obtained after the images had stabilized.

27. A. Polyanskii et al., J. Less Common Metals **164**, 1300 (1990).

28. Reported J_c values[1,2,9,32] for twinned single crystals at similar conditions are in the range of 0.5 x 10^4 to 5.6 x 10^4 A/cm^2.

29. J. P. Rice and D. M. Ginsberg, J. Cryst. Growth **109**, 432 (1991).

Fig. 1 Specimen 1 (single crystal). a) Polarized light optical micrograph showing the twin structure

consisting of polytwin blocks. b-d) Magneto-optical images of flux penetration in crystal 1 at

35 K for H_a = 12 mTesla (b), H_a = 19 mTesla (c) and H_a = 30 mTesla (d). e) Contour map

of image d showing lines of equal magnetic induction (difference between lines is ~ 3.5

mTesla.) Yellow areas in images b-d denote flux penetration; brown regions correspond to

zero magnetic induction; and the zig-zag lines are magnetic domain boundaries in the garnet

indicator film. Segments AB and BC in the line shown on the contour map lie along and

across TBs respectively.

Fig. 2 Specimen 3 (single crystal). a) Polarized light optical micrograph showing regions of varying

twin density. b-d) Magnetic induction profiles taken at 53 K and H_a = 14 mTesla in direction

1 in an untwinned region (b), direction 2 in a lightly twinned region (c), and direction 3 in a

heavily twinned region (d). The profiles were measured along segments 125 μm in length.
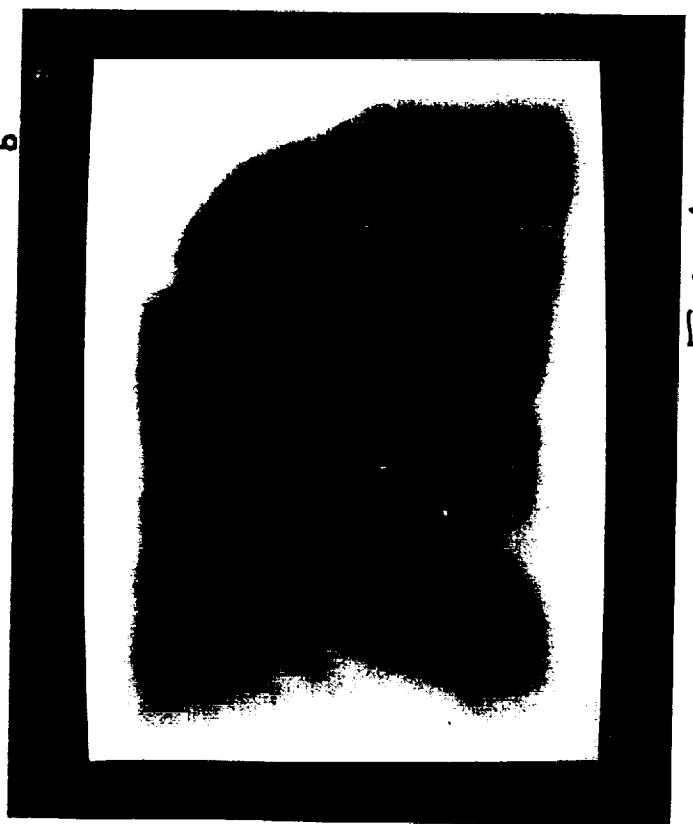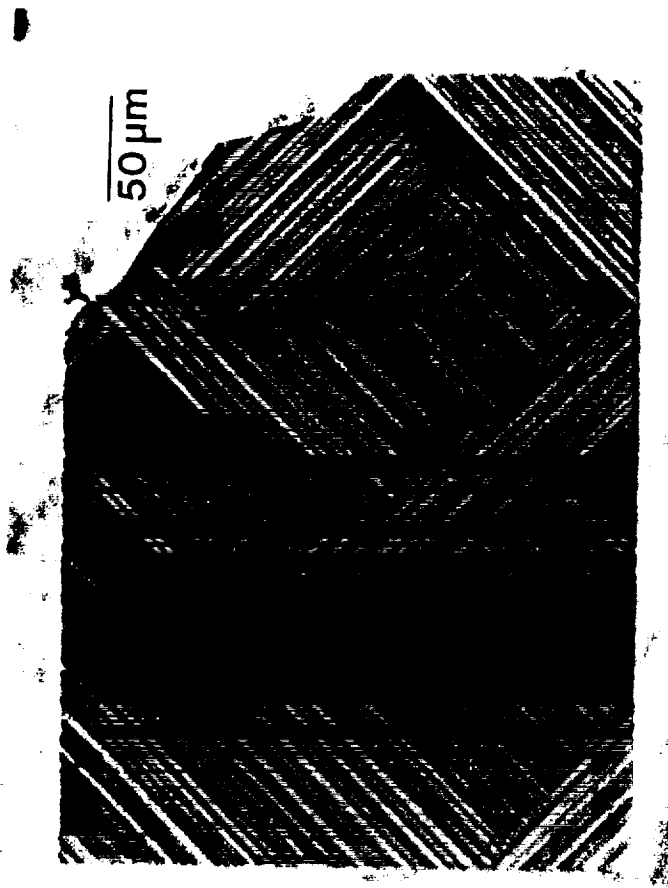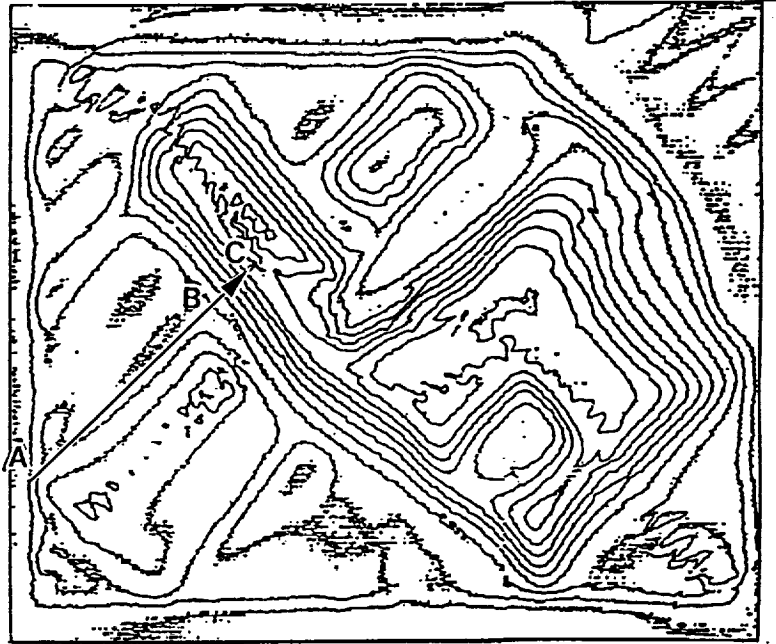
50 μm

a

b

c

d

FIG. 1.

Fig. 1c

Fig. 1 Specimen 1 (single crystal). a) Polarized light optical micrograph showing the twin structure consisting of polytwin blocks. b-d) Magneto-optical images of flux penetration in crystal 1 at 35 K for H_a = 12 mTesla (b), H_a = 19 mTesla (c) and H_a = 30 mTesla (d). e) Contour map of image d showing lines of equal magnetic induction (difference between lines is ~ 3.5 mTesla.) Yellow areas in images b-d denote flux penetration; brown regions correspond to zero magnetic induction; and the zig-zag lines are magnetic domain boundaries in the garnet indicator film. Segments AB and BC in the line shown on the contour map lie along and across TBs respectively.